GCOM-C/SGLI Land Atmospheric Correction Algorithm

Hiroshi Murakami,
JAXA/EORC
Aug. 2021 (v3.00: Main revisions of Ver. 3 is underlined)

1 Overview of Algorithm

1.1 Definition of GCOM-C atmospheric corrected land surface reflectance (RSRF) product

- Surface reflectance of solid or liquid structures on the ground which includes canopy, snow, and water. Light scattering and absorption of atmospheric molecules and aerosol particles are corrected from clear sky top of atmosphere (TOA) reflectance. In the water area, it is the water-leaving reflectance, i.e., the water surface reflection is subtracted.
- Directional dependency is not corrected for the snapshot (one-day) product, and the directionality of satellite viewing angles is corrected for the 8-day and monthly land surface reflectance products (it corresponds to nadir reflectance under the clear sky solar condition at the observation solar angles).
- Slope effect correction, which normalizes solar irradiance change due to the land-surface slope, has been investigated, however, it is not implemented by considering effectiveness currently.
- The SGLI atmospheric correction over water areas is similar with the ocean color algorithm which mainly uses near-infrared and red channels to correct the aerosol reflectance and the water surface reflection is subtracted with the atmosphere reflectance. The differences between the RSRF of the water surface and the normalized water-leaving radiance (NWLR: the ocean color product) are the unit of NWLR is W/m^2/str/μm or /str (remote sensing reflectance, Rrs) but unit of RSRF is non-dimension, and the directionality (BRDF) is corrected for NWLR and not corrected for the daily RSRF (consistent with the daily land surface reflectance). Approximately RSRF can be converted to Rrs (or NWLR) by the following equation:

  $Rrs \cong RSRF / \pi$

  $NWLR \cong RSRF / \pi \times F_0$

  (F_0: SGLI channel weighted solar irradiance, see Table 1)

1.2 Development strategy (discussed in the atmospheric correction workshop in Sep. 2012)

- The algorithm is mainly developed by JAXA/EORC through integration of knowledge about the atmosphere (aerosol scattering and absorption, and radiative transfer modeling), the land surface (spectral reflectance and bidirectional reflectance), and cloud (and snow cover) area detection in collaboration with PI groups.
- The algorithm considers consistency (e.g., candidate aerosol model and BRDF) with downstream products (land and atmosphere products) and sensor calibration characteristics including vicarious calibration by using other satellite sensors and in-situ observation, and calibration corrections.
- In-situ validation data (BRDF, solar irradiance, and aerosols) have been provided by land-PIs (Honda, Chiba Univ., Nasahara, Tsukuba Univ., and so on). Atmospheric parameters have been obtained

simultaneously as much as possible in collaboration with the atmosphere PIs.

1.3 Function and characteristics

- Output land surface reflectance by subtracting atmospheric molecules and aerosols from TOA radiance (reflectance) in the daytime clear sky areas.
- Reflectance is one at the satellite-solar geometric condition by consideration of land-surface BRDF estimated by using multiple-day's input (LTOA) data.

1.4 Interface in the GCOM-C processing flow

- Multiple day (32 days) precise geometric corrected tile-mapped TOA radiance (reflectance) data (LTOAQ) is used as the input.
- Dynamic look-up table (LUT) is used to use previous day's BRDF estimation for the aerosol correction.
- Output surface reflectance data (RSRF) is averaged for 8-day and monthly in the level-3 processing.

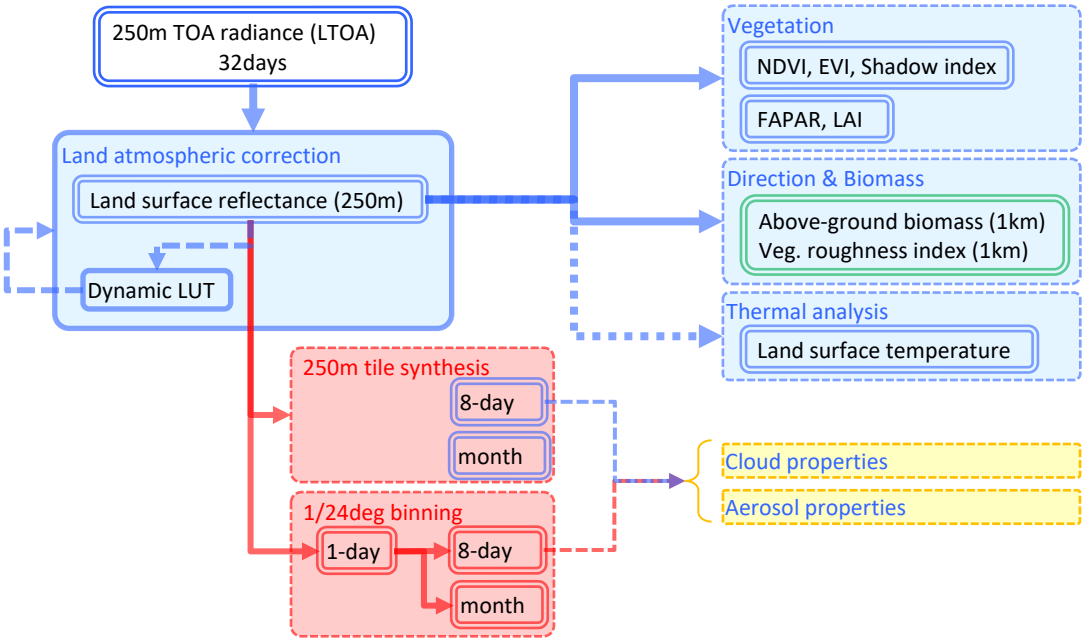

Fig. 1 Operation flow around the GCOM-C Land Atmospheric Correction

1.5 New development

- This BRDF estimation scheme using the multiple day data has been developed by several studies by MODIS (Lyapustin et al., 2012) and higher-resolution sensors (Hajj et al., 2008, Hagolle et al., 2008), however it is not usual being the standard product because of estimation instability and long processing time. The SGLI algorithm realized the multiple day processing as the standard product by reducing the processing time by the simplified data flow and running archive of the LUTs.

1.6 Development history

- 2012/9: development strategy was discussed in the atmospheric correction workshop
- 2015/1/13：Deriver the first version code

- 2015/07/20: bug fix in lut_d/RSRF/*BRDFQ output and observation time handling
- 2015/09/03: bug fix in dataset name: Sensor_***_TI -> Sensor_***_IR
- 2016/01/29 (v005): change NG to Poor when n_in==0
- 2017/01/31 (v006): revision of the multi-day estimation module, and reduce the processing time, including correction of center-wavelength shift and slope effect
- 2018/07/31 overall revision and bug-fix of main code:
  - tuning of cloud detection thresholds
  - lut is made by pstar4; ALOS DEM files is added for LTOAF
  - adjustment to the post-launch LTOAQ and LTOAF values and format
  - processing line-block is changed to 160 lines
  - saturation recovery & saturation recovery flag
  - Obs_time_IR is deleted as same as LTOAQ/K
- 2018/10/23 (1.00 000.00)
  - revision of NDVI->ref relationship by Fuji Hokuroku in 2016-2018
  - revision of the conversion weights
  - Byte size of BRF1,2 coefficients of lud_d file was changed from 2byte to 1byte (to reduce the lut_d files)
  - Attribute: Photosynthetically Active Radiation -> Daily Photosynthetically Active Radiation
  - Attribute: Surface reflectance of VN08 co-registered for VN08 -> Surface reflectance of VN08 co-registered for PI01
  - Attribute: Surface reflectance of VN11 co-registered for VN11 -> Surface reflectance of VN11 co-registered for PI02
  - allow LTOA version -0~-5 as the input files
- 2018/11/06 (1.01 001.00) [Ver.1]
  - Set error values for the saturation of VN04 and VN06
  - if(slopr0(nb,k).ne.slopr(nb,k)) then
    -> if((slopr0(nb,k).ne.slopr(nb,k)).or.(offsr0(nb,k).ne.offsr(nb,k))) then
- 2019/06/17 (1.01 002.00)
  - JMA ozone data is used
- 2019/08/27 (1.01 002.01)
  - wrong explanation, " (from the earth surface)" is deleted in Data_description of zenith angles
- 2020/01/04 (2.00 000.00)
  - Flag definition is revised including the additional tests for the polarization channels
  - BRDF of VN08P and VN11P is calculated with PI01 and PI02 respectively
  - bug fix: rea->abs(rea) for BRF kernel calculation
  - hotspot of BRF function is moderated (hspot=1.0 -> 5.0)
  - vical coeffs are revised to adjust with the Ver.2 L1B which is consider the temporal gain change derived from the moon calibration

- 2020/02/27 (2.00 000.01)
  - bug fix: uninitialized parameter "vgi" in the subroutine "brdf_multiday"
  - file list is input from the "main" to the "brdf_multiday"
  - Sortwave irradiance (/Image_data/SWR) is stored in output file
  - revise ocean surface reflectance (rs2) recovery for the "cal_par"
- 2020/03/25 (2.00 000.02) [Ver.2]
  - add nrt processing with today's lut_d ($3="-2")
  - bug fix: add brfk recovery under clouds for reflectance of the daily processing
  - Absorption calculation for SWR is revised in "cal_par"
  - Set input lut_d information in attribute of /Processing_attributes/LUT_file
  - 2018/12/31 lut_d is used for the first day 2018/01/01 data
  - use input days for Processing_result (ninlst>ndyl1*0.9;qidx='Good';else;qidx='Fair')
- 2021/07/26 (3.00 000.04) [Ver.3]
  - Output polarization reflectance at PL01 and PL02
  - Flat ocean surface aerosol LUTs are used for the ocean areas
  - probably cloud flag is reduced by changing to cloud area (NP) and recovery of bright area (PL)
  - recover cloud detection when TI01 detector anomaly with high TI01 range
  - Rayleigh LUT of center wavelength shift is off, and use a nominal center wavelength LUT
  - add the correction of the offset temporal change of the old version Level-1B (Ver.1 VNR radiance and Ver 2003 POL radiance)
  - reduce sample if NP fine days>=10 & PL fine days>=6 & the day is not the clearest day
  - few-samples flag is only available when bit0=0 (data are available)
  - The weighting function of the optimal Rs search is revised (mixed with lud_d)
  - bug fix in the POL sample count in the multi-day processing
  - bug fix in reading the pre-day's BRDF data

2 SGLI Land Atmospheric Correction Algorithm

2.1 Algorithm flow

- Input precise geometric corrected TOA reflectance data (LTOA) of 32 (variable) days. Both 250-m LTOA (LTOAQ) and 1-km LTOA (LTOAK) can be inputted (LTOAK input is not for the standard processing)
- Previous day's BRDF LUT (dynamic LUT) is inputted, and current day's BRDF LUT is outputted.
- Current day land surface reflectance (RSRF) is produced by the current day LTOA and current day BRDF LUT.
- The outputted RSRF is averaged for 8-day and monthly in the level-3 processing.
- The 8-day data is used for the atmospheric product processing

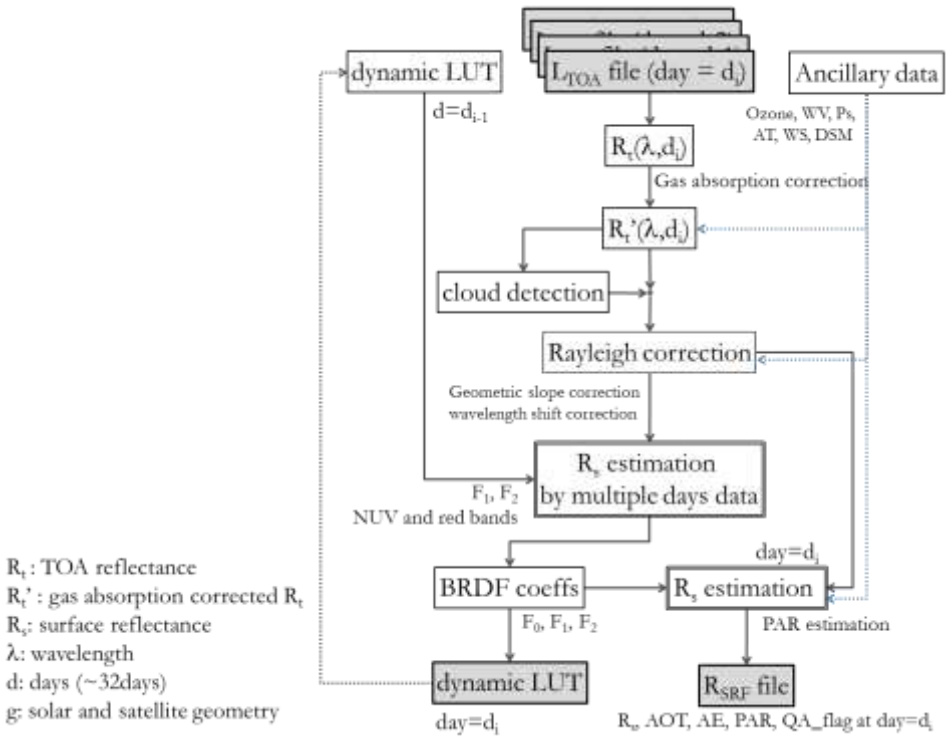

Figure 2 Overall flow of SGLI land atmospheric correction

2.2 Radiance to reflectance

TOA radiance L_{TOA} is converted to TOA reflectance ρ_{TOA} for each SGLI channel (λ)

$$\rho_{TOA}(\lambda) = \pi L_{TOA}(\lambda)\, d^2 / (F_0(\lambda) \cos(\theta_0))$$

where d is distance between the sun to the earth (1: 1AU), $F_0(\lambda)$ is SGLI-channel weighted solar irradiance (calculated by using Thuillier 2003), θ_0 is solar zenith angle.

Table 1 SGLI-band weighted center wavelength (λ_c) and solar irradiance (F_0)

band	λ_c (nm)	F_0 ($Wm^{-2}\mu m^{-1}$)	Min λ_c (nm)	F_0 ($Wm^{-2}\mu m^{-1}$)	Max λ_c (nm)	F_0 ($Wm^{-2}\mu m^{-1}$)
VN01	380.03	1092.14	379.80	1093.97	380.24	1090.67
VN02	412.51	1712.15	412.11	1710.45	412.68	1712.86
VN03	443.24	1898.32	442.96	1891.31	443.57	1906.81
VN04	489.85	1938.46	489.60	1937.76	490.39	1941.65
VN05	529.64	1850.96	529.47	1850.33	530.09	1852.37
VN06	566.15	1797.13	565.76	1797.75	566.56	1796.60
VN07	672.00	1502.55	671.73	1503.26	672.61	1500.80
VN08	672.10	1502.30	671.89	1502.87	672.67	1500.65
VN09	763.07	1245.45	762.35	1247.82	763.58	1243.79
VN10	866.76	956.34	866.11	955.99	867.48	956.52
VN11	867.12	956.62	866.40	956.29	867.90	956.71
PL01	671.89	1503.59	671.89	1503.60	673.10	1499.84
PL02	866.18	956.92	865.85	956.68	866.63	957.13
SW01	1054.99	646.54	NA	NA	NA	NA
SW02	1385.35	361.24	NA	NA	NA	NA
SW03	1634.51	237.58	NA	NA	NA	NA
SW04	2209.48	84.25	NA	NA	NA	NA
TI01	10792.98	0.00	NA	NA	NA	NA
TI02	11956.28	0.00	NA	NA	NA	NA

2.3 Gas absorption correction

Absorption coefficients of H_2O, O_3, and O_2 are calculated by PSTAR4 (Ota et al., 2010) by the following equation.

$$\rho_{TOA}(\lambda)' = \rho_{TOA}(\lambda) / (t_g(\lambda)^{am})$$

$$t_g(\lambda) = \exp\{ -(k_{oz0}(\lambda) + k_{oz1}(\lambda) \times (oz - oz_0)^{\alpha}) \times (oz - oz_0)$$
$$-(k_{wv0}(\lambda) + k_{wv1}(\lambda) \times (wv - wv_0)^{\alpha}) \times (wv - wv_0)$$
$$-(k_{ox0}(\lambda) + k_{ox1}(\lambda) \times (P - P_0)^{\alpha}) \times (P - P_0) \}$$

$$am = 1/\cos(\theta) + 1/\cos(\theta_0)$$

oz, wv, and P are column ozone (DU), column water vapor (mm), and relative surface pressure (1.0: 1013.25hPa). oz_0=343.79 DU, wv_0=14.186 mm, P_0=1013.25 hPa. θ is satellite zenith angle.

Table 2 Gas absorption coefficients of SGLI channels

gas	Channel	λc min			λc max		
		0	1	a	0	1	a
k_{wv}	VN01	1.5445E-06	0.0000E+00	0.00	1.48620E-06	0.00000E+00	0.00
	VN02	9.4948E-07	0.0000E+00	0.00	1.00540E-06	0.00000E+00	0.00
	VN03	3.1314E-05	0.0000E+00	0.00	3.20730E-05	0.00000E+00	0.00
	VN04	1.0517E-05	0.0000E+00	0.00	1.02670E-05	0.00000E+00	0.00
	VN05	1.6059E-05	0.0000E+00	0.00	1.79770E-05	0.00000E+00	0.00
	VN06	1.1847E-04	0.0000E+00	0.00	1.25530E-04	0.00000E+00	0.00
	VN07	5.9118E-05	0.0000E+00	0.00	5.21940E-05	0.00000E+00	0.00
	VN08	5.7061E-05	0.0000E+00	0.00	5.15330E-05	0.00000E+00	0.00
	VN09	2.1217E-06	0.0000E+00	0.00	1.39310E-06	0.00000E+00	0.00
	VN10	8.8784E-05	0.0000E+00	0.00	7.31440E-05	0.00000E+00	0.00
	VN11	8.4187E-05	0.0000E+00	0.00	6.97610E-05	0.00000E+00	0.00
	PL01	4.7346E-05	0.0000E+00	0.00	4.21620E-05	0.00000E+00	0.00
	PL02	8.3032E-05	0.0000E+00	0.00	7.26590E-05	0.00000E+00	0.00
	SW01	4.0931E-05	0.0000E+00	0.00			
	SW02	-2.5585E-01	1.4719E+00	-0.32			
	SW03	4.3975E-03	-2.8813E-03	0.06			
	SW04	1.7986E-02	-1.1061E-02	0.08			
k_{ox} (O2)	VN01	1.6224E-03	0.0000E+00	0.00	1.62430E-03	0.00000E+00	0.00
	VN02	4.0746E-05	0.0000E+00	0.00	4.28740E-05	0.00000E+00	0.00
	VN03	4.5989E-04	0.0000E+00	0.00	4.83160E-04	0.00000E+00	0.00
	VN04	2.1982E-04	0.0000E+00	0.00	1.77910E-04	0.00000E+00	0.00
	VN05	1.1559E-03	0.0000E+00	0.00	1.16790E-03	0.00000E+00	0.00
	VN06	5.3377E-03	0.0000E+00	0.00	5.81480E-03	0.00000E+00	0.00
	VN07	1.1843E-03	0.0000E+00	0.00	1.72480E-03	0.00000E+00	0.00
	VN08	1.2444E-03	0.0000E+00	0.00	1.73980E-03	0.00000E+00	0.00
	VN09	3.0435E-02	2.8313E-01	-0.60	3.13240E-02	2.85120E-01	-0.60
	VN10	4.3529E-05	0.0000E+00	0.00	4.53640E-05	0.00000E+00	0.00
	VN11	4.3813E-05	0.0000E+00	0.00	4.74650E-05	0.00000E+00	0.00
	PL01	1.3550E-03	0.0000E+00	0.00	2.22670E-03	0.00000E+00	0.00
	PL02	4.2436E-05	0.0000E+00	0.00	4.23090E-05	0.00000E+00	0.00
	SW01	8.5098E-03	0.0000E+00	0.00			
	SW02	4.0890E-04	0.0000E+00	0.00			
	SW03	4.9989E-07	0.0000E+00	0.00			
	SW04	6.8205E-08	0.0000E+00	0.00			
k_{oz}	VN01	9.0074E-09	0.0000E+00	0.00	7.68290E-09	0.00000E+00	0.00
	VN02	2.4232E-07	0.0000E+00	0.00	2.59410E-07	0.00000E+00	0.00
	VN03	2.9846E-06	0.0000E+00	0.00	3.06890E-06	0.00000E+00	0.00
	VN04	2.0569E-05	0.0000E+00	0.00	2.08290E-05	0.00000E+00	0.00
	VN05	6.5299E-05	0.0000E+00	0.00	6.61650E-05	0.00000E+00	0.00
	VN06	1.1405E-04	0.0000E+00	0.00	1.15180E-04	0.00000E+00	0.00

	VN07	4.2992E-05	0.0000E+00	0.00	4.22160E-05	0.00000E+00	0.00
	VN08	4.2845E-05	0.0000E+00	0.00	4.21660E-05	0.00000E+00	0.00
	VN09	6.7584E-06	0.0000E+00	0.00	6.65850E-06	0.00000E+00	0.00
	VN10	1.9868E-06	0.0000E+00	0.00	1.83670E-06	0.00000E+00	0.00
	VN11	1.9547E-06	0.0000E+00	0.00	1.79090E-06	0.00000E+00	0.00
	PL01	4.2834E-05	0.0000E+00	0.00	4.17610E-05	0.00000E+00	0.00
	PL02	2.0130E-06	0.0000E+00	0.00	1.92160E-06	0.00000E+00	0.00
	SW01	8.0493E-08	0.0000E+00	0.00			
	SW02	3.5094E-09	0.0000E+00	0.00			
	SW03	0.0000E+00	0.0000E+00	0.00			
	SW04	0.0000E+00	0.0000E+00	0.00			

2.4 Cloud detection

Cloud detection algorithms of GCOM-C algorithms are developed by sharing knowledge of the cloud optical properties mainly studied by the atmosphere group, and implemented in the each algorithm. Simple decision tree will be used for the first version of the land atmospheric correction algorithm.

2.4.1 Decision tree

Following decision tree is applied for solar zenith angle $\theta_0 < 76$ degrees.

if((rc443<rt443) & (rc868≤0.08) & (sst>-5.0) & (btd<5.5) & ((btd>-1.5) | (sst>20)) & ((elv<1) | ((elv<200) & (vgi<0.1)))) then
→ clear ocean
elseif((rc443<rt443) & (rc868>0.08) & (rc868>1.1×rc443) & (btd<5.5) & ((btd>-1.5) | (sst>20)) & (elv>0)) then
→ clear land
elseif((rc443≥0.25) & (rc1640<rc443×rsnow) & (rc1640<rc1050×fsnow) & (rc1380/rs1380<r1380) & (sst<273.15) & (btd<5.0) & (sgr<0.01) & (Ta<278.15)) then
→ clear snow
else
→ cloud
endif

2.4.2 Parameters

- TOA reflectance after gas absorption, rc443, 673, 868, 1050, 1640, 1380 nm
- bright temperature of 11μm band, BT11
- bright temperature of 12μm band, BT12
- bright temperature difference, btd
  btd = BT11–BT12
- air temperature, Ta [K]
- approximate sea surface temperature, sst [K]
  $sst = c_{sst}(1) + c_{sst}(2) \times BT11 + c_{sst}(3) \times btd + c_{sst}(4) \times btd \times pl$
  c_{sst} =(/-1.5258, 1.0054, 2.4108, 0.56367/) ! SST by BT for SGLI (by pstar)
  pl : path length calculated by $1.0/\cos(\theta)-1.0$
  θ : satellite zenith angle
- approximate column water vapor, wvp [mm]
  $wvp = wvc(1) \times btd + wvc(2) \times btd^2$
  wvc =(/11.4821, 5.41933/) ! WV by btd for SGLI (by pstar)
- btd estimated by ancillary column water vapor, bte [K]
  $dte = btc(1) \times wv + btc(2) \times wv^2$
  btc =(/0.063033,-0.00037827/) ! btd by WV for SGLI (by pstar)

- 1380 nm reflectance without water vapor absorption calculated by interpolation of 1050 nm and 1640 nm, rs1380
  rs1380 =(rc1050× (1640−1380)+rc1640× (1380−1050))/(1640−1050)

- threshold of transmittance of 1380nm, r1380

```
if( ( |rlat|<snowlat) | ((elv<1500) & (|rlat|<35)) ) then
  r1380=0.95-0.90×epr^2                ! tropical
else
  r1380 =1.0 –0.90×epr^2
endif
   epr: atmospheric pressure /1013.25 (1.0: 1013.25hPa)
```

- distribution latitude range of snow areas, snowlat [deg]

```
snowlat=40 –elv×0.01
   elv: land surface elevation [m]
```

- threshold of 1640nm/1050nm ratio, fsnow

```
fsnow=0.7
```

- threshold of 1640nm/443nmratio, rsnow

```
if(lat<-60) then                          ! Antarctic
  rsnow=0.10
elseif((elv>1000) & (lat> 60) & (lon>-65) & (lon<-20)) then      ! GreenLD
  rsnow=0.10
elseif( |lat| <snowlat) then                        ! tropical
  rsnow=0.20
elseif((elv<1500) & (|lat| <35)) then             ! tropical
  rsnow=0.10
else
  rsnow=0.28
endif
   lat: latitude [deg]
   lon: longitude [deg]
```

- threshold of 443nm reflectance, rt443

```
if(rc868≤0.08) then
  rt443=0.35
else
  rt443=0.35–vgi×0.20
  if(rt4430<0.16) rt443=0.16
  if(rt443>0.35) rt443=0.35
endif
```

- vegetation index, vgi

```
   vgi=(rc868–rc673)/(rc868+rc673)
```

2.5 Surface reflectance

2.5.1 Minimum reflectance

Minimum reflectance (a maximum NDVI sample between the 1st and 2nd minimum reflectance samples to avoid shadows) after the molecular reflectance and transmittance (without aerosols), $r_s^{min}(\lambda)$ is used as initial values and index calculations.

2.5.2 Near-UV and red band reflectance

Near-UV and red band reflectance, $r_s^{sim}(\lambda)$ is estimated by the NDVI calculated from $r_s^{min}(\lambda)$. $r_s^{sim}(\lambda)$ is supplementary used for candidate $r_s(\lambda)$ in the multi-temporal variation scheme.

$r_s^{sim}(\lambda)=b_0(\lambda) +b_1(\lambda)$ NDVI

Table 3 Coefficients of surface reflectance estimation by NDVI

λ [nm]	b0	b1
380.1	0.0355	-0.0272
412.6	0.0422	-0.0338
443.3	0.0474	-0.0377
672.2	0.1257	-0.1237

r_s^{sim} is used if NDVI>0.35, and the 2nd minimum reflectance is used if NDVI<0.15, and linearly transitioned when NDVI from 0.15 to 0.35.

2.5.3 Multi-temporal variation scheme

This scheme estimate the surface reflectance Rs(λ) by using the general characteristics of temporal variation of surface reflectance is small and temporal variation of atmosphere is large.

Rs(λ) is searched as minimizing temporal variation of Rs(λ) at multiple λ in about a month by testing aerosol models (M) and optical thickness (τ_a).

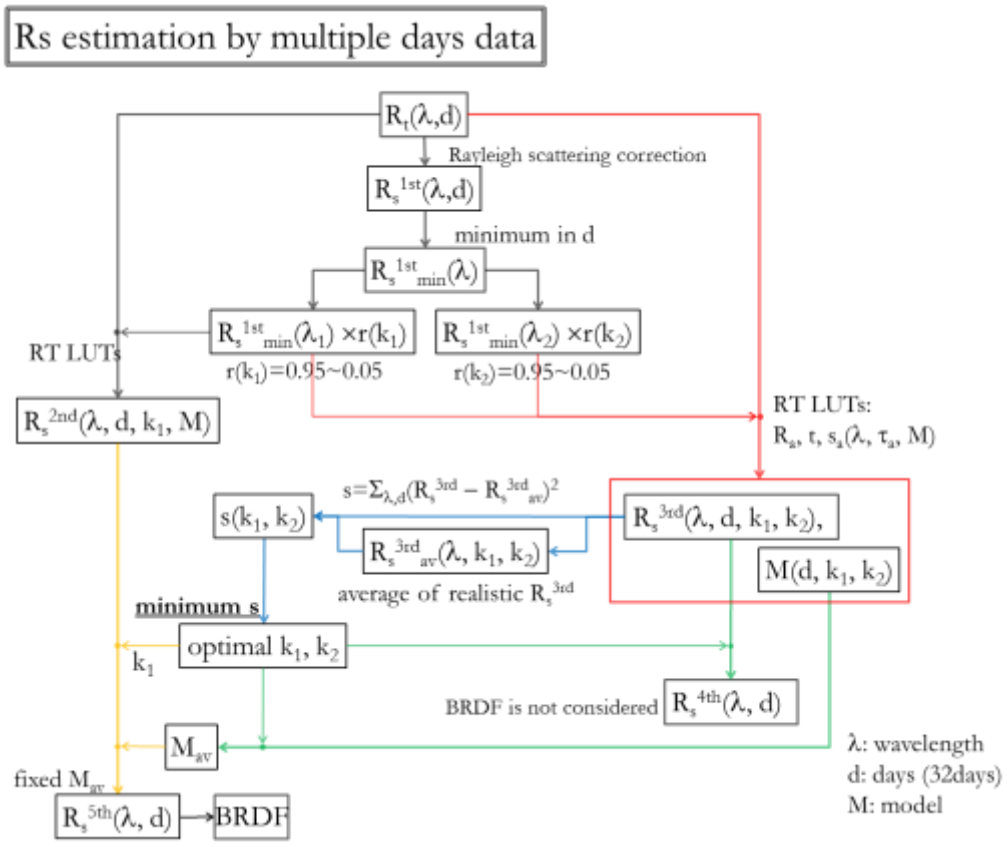

Figure 3 Flow of the multi-temporal variation surface reflectance estimation algorithm

(1) preset several candidate surface reflectance at the base band (λ_{blue}), $Rs(\lambda_{blue})_j$, and estimate τ_a at each M

$$R_t(\lambda) / t' - R_r(\lambda) = R_a(\lambda) + (t_0(\lambda)t_1(\lambda) \times Rs(\lambda)) / (1 - S_a(\lambda) \times Rs(\lambda)) \quad (1)$$

(2) M is calculated by presetting surface reflectance at the reference band $Rs(\lambda_{red})$

(3) surface reflectance at the other bands $Rs(\lambda)_j$ is calculated by the spectral relationship of

$R_a(\lambda), t_0(\lambda) t_1(\lambda), S_a(\lambda)$ of the loop-up table

(4) Optimal Rs(λ) is selected from the $Rs(\lambda)_j$ (j = 1-32 days) to minimize temporal variation of Rs(λ) at multiple bands λ.

(5) the first to the nineth temporally newest clear samples are selected for the BRDF processing.

(6) BRDF is calculated from Rs(λ) calculated by $Rs(\lambda_{blue})$ and mean of M

2.6 Candidate aerosol model

Aerosol models, M, are constructed by mixing the tropospheric and sea-salt particle type aerosols. It is made as look-up tables which include TOA reflectance at solar and satellite geometries, transmittance, aerosol optical thickness, spherical albedo

The aerosol models (particle size distribution, particle shape, and refractive index) are consistent with the models used in the atmosphere aerosol algorithms.

2.7 Other corrections

2.7.1 Altitude correction

$t_{d0n}=t_{d0}(b,1,1)^{(epr1-1.)}$

$t_{d1n}=t_{d1}(b,1,1)^{(epr1-1.)}$

$r_{rL}(b)= r_{rL}(b) \times Prs$! land

$r_{rO}(b)= r_{rO}(b) \times Prs$! ocean

$s_a(b,t,m)=s_a(b,t,m) \times Prs$

$td0(b,t,m)=td0(b,t,m) \times t_{d0n}$

$td1(b,t,m)=td1(b,t,m) \times t_{d1n}$

2.7.2 molecule scattering correction

$r_{rc}(b) = r_t(b) - r_r(b)$

$r_{s0}(b) = r_{rc}(b) / (t_{d0}(b,1,1) \times t_{d1}(b,1,1) + r_{rc}(b) \times s_a(b,1,1))$

2.7.3 BRF correction

$$\boldsymbol{R(\theta_0, \theta_1, \varphi) = k_0 + k_1 \times F_1(\theta_0, \theta_1, \varphi) + k_2 \times F_2(\theta_0, \theta_1, \varphi)}$$

k_0= *Nadir reflectance*

$$F_1=((\pi - \varphi)\times cos(\varphi)+sin(\varphi)) \times tan(\theta_0) \times tan(\theta_1)/(2 \times \pi) - (tan(\theta_0)+ tan(\theta_1)+ \Delta)/\pi$$

$$F_2=(4/3/\pi)/(cos(\theta_0)+cos(\theta_1)) \times((\pi /2-\alpha) \times cos(\alpha)+sin(\alpha)) \times(1+1/(h+ \alpha /(1.5/180\times\pi))) - 1/3$$

$\Delta=sqrt(tan(\theta_0)^2+tan(\theta_1)^2 - 2 \times tan(\theta_0) \times tan(\theta_1) \times cos(\varphi))$

$\alpha=acos\{cos(\theta_0) \times cos(\theta_1) + sin(\theta_0) \times sin(\theta_1) \times cos(\varphi)\}$

θ_0: *solar zenith,*

θ_1: *satellite zenith,*

φ: *ABS(relative azimuth),*

α: *scattering angle*

$h=5.0$ (The parameter *h* is originally 1.0; it set to 5.0 for the Ver. 2 to be stable regression)

2.7.4 slope correction (not applied for the current version)

$$R_t/t_g = R_a + (r_{slp}\, t_0\, t_1\, A_s) / (1 - S_a\, A_s)$$

$$A_s = (R_t/t_g - R_a) / (r_{slp}\, t_0\, t_1 + (R_t/t_g - R_a)\, S_a)$$

$$r_{slp} = ((1 - r_{dir})\, cos(\theta_{sun}) + r_{dir}\, cos(\theta_{slp})) / cos(\theta_{sun})$$

$$\theta_{slp} = sin(\theta_{sun})\ cos(\phi_{sun})\ sin(\theta_{slp})\ cos(\phi_{slp}) + sin(\theta_{sun})\ sin(\phi_{sun})\ sin(\theta_{slp})\ sin(\phi_{slp}) + cos(\phi_{sun})\ cos(\phi_{slp})$$

$$r_{dir} = t_b / t_{dif}$$

$$t_b = exp(-(\tau_m + \tau_a))$$

$$t_{dif} = exp(-(\tau_{mb} + (b_{ba0} + b_{ba1}\,\alpha)\,\tau_a))$$

$$\tau_a = \tau_{a0}\,(\lambda/500\mathrm{nm})^{\alpha}$$

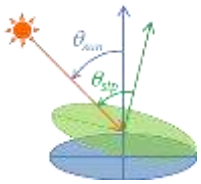

2.7.5 center-wavelength correction (not applied for the at-launch version)

The center wavelength is calculated by the center-wavelength shift mode from the ground tests using relative pixel position which is calculated by the pixel address and telescope information (/Geometry_data/Cross_track_section_flag) and satellite zenith angle.

VNR-NPL: $rpix = 9.61898e\text{-}01 - 3.73884e\text{-}02 \times \theta + 3.97139e\text{-}05 \times \theta^2$

VNR-NPN1 : $rpix = -3.73684e\text{-}02 \times \theta - 4.63678e\text{-}05 \times \theta^2$

VNR-NPN2 : $rpix = 3.73684e\text{-}02 \times \theta + 4.63678e\text{-}05 \times \theta^2$

VNR-NPR : $rpix = -9.61898e\text{-}01 + 3.73884e\text{-}02 \times \theta - 3.97139e\text{-}05 \times \theta^2$

VNR-PL1 : $rpix = -8.65696e\text{-}03 \times \theta - 8.81878e\text{-}05 \times \theta^2$

VNR-PL2 : $rpix = 8.65696e\text{-}03 \times \theta + 8.81878e\text{-}05 \times \theta^2$

θ: satellite zenith angle of VNR-NP (deg)

$\lambda_c[nm] = c0 + c1*X + c2*X^2 + c3*X^3 + c4*X^4$

X (= -0.5 ~ +0.5): (pixels - center_pixel)/pixel_length

pixels: 1~pixel_length at a telescope

pixel_length=1500 (VNR-NP 250m),

pixel_length=857 (VNR-PL)

c0: center wavelength at the telescope center (X=0)

Molecular scattering table and gas absorption table of minimum and maximum center-wavelength are linear interpolated by the calculated center wavelength.

Table 4 Coefficients of SGLI center wavelength shift

Band	c0	c1	c2	c3	c4	RgErr[nm]	Ave[nm]	Min[nm]	Max[nm]
VNL01	3.7983E+02	-2.0654E-01	4.0953E-01	7.6962E-01	-7.5110E-01	0.005	379.85	379.80	379.91
VNL02	4.1235E+02	1.1515E-01	-7.2607E-02	5.3384E-01	-2.0197E+00	0.005	412.31	412.11	412.38
VNL03	4.4337E+02	9.0581E-02	6.3376E-01	5.5982E-02	7.0385E-02	0.004	443.43	443.37	443.57
VNL04	4.8966E+02	-3.0622E-01	3.3672E-01	4.5020E-01	-3.9824E-01	0.005	489.69	489.60	489.81
VNL05	5.2952E+02	-3.5294E-01	9.6784E-01	-3.1234E-01	1.9387E+00	0.011	529.62	529.47	530.08
VNL06	5.6589E+02	2.4046E-01	8.7851E-01	6.2411E-01	-2.7019E+00	0.008	565.93	565.76	566.12
VNL07	6.7184E+02	-3.4264E-01	7.7027E-01	-6.1871E-01	5.8120E+00	0.020	671.98	671.81	672.61
VNL08	6.7201E+02	-4.1357E-01	6.0967E-01	1.8496E-01	5.3048E+00	0.018	672.13	671.96	672.65
VNL09	7.6327E+02	3.1900E-01	-2.6370E+00	-1.6204E+00	-4.7683E+00	0.008	762.96	762.35	763.28
VNL10	8.6738E+02	1.8538E+00	-1.3750E+01	-1.2301E+01	4.8520E+01	0.046	866.83	866.23	867.48
VNL11	8.6759E+02	1.8948E+00	-1.3941E+01	-1.2742E+01	4.8163E+01	0.042	867.02	866.40	867.70
VNN01	3.8001E+02	1.7104E-01	2.9402E-01	-6.5029E-01	-6.9351E-01	0.005	380.03	379.99	380.08
VNN02	4.1257E+02	1.6869E-01	-2.2033E-01	4.3098E-01	-1.9828E+00	0.008	412.52	412.28	412.60
VNN03	4.4316E+02	-9.9156E-02	7.1108E-01	-1.6487E-02	4.1156E-01	0.005	443.23	443.16	443.40
VNN04	4.8983E+02	2.8187E-01	2.9698E-01	-3.6911E-01	-5.8977E-01	0.005	489.85	489.77	489.97

VNN05	5.2952E+02	3.9348E-01	8.8587E-01	2.7552E-01	2.0914E+00	0.010	529.63	529.48	530.09
VNN06	5.6613E+02	2.9743E-01	7.9222E-01	4.1063E-01	-2.9697E+00	0.007	566.16	565.96	566.34
VNN07	6.7182E+02	3.8590E-01	1.2226E+00	-2.3696E-02	3.8871E+00	0.022	671.97	671.76	672.55
VNN08	6.7194E+02	4.3907E-01	7.5132E-01	2.2127E-02	5.3565E+00	0.018	672.08	671.89	672.66
VNN09	7.6342E+02	-3.1793E-01	-2.5845E+00	1.6389E+00	-4.8441E+00	0.008	763.12	762.51	763.43
VNN10	8.6730E+02	-1.7540E+00	-1.3713E+01	1.2056E+01	4.8410E+01	0.045	866.76	866.18	867.43
VNN11	8.6767E+02	-1.8758E+00	-1.3568E+01	1.2824E+01	4.7018E+01	0.032	867.12	866.50	867.81
VNR01	3.8020E+02	-1.4418E-01	2.5644E-01	6.5340E-01	-9.4438E-01	0.006	380.21	380.18	380.24
VNR02	4.1265E+02	2.0817E-01	-3.2323E-01	3.4006E-01	-1.7034E+00	0.006	412.60	412.34	412.68
VNR03	4.4296E+02	1.0681E-01	8.1284E-01	-3.6629E-02	7.1595E-01	0.004	443.04	442.96	443.24
VNR04	4.9032E+02	-2.2237E-01	1.0639E-02	2.1432E-01	-5.0950E-01	0.007	490.31	490.21	490.39
VNR05	5.2955E+02	-4.1437E-01	9.1150E-01	-1.2109E-01	1.6420E+00	0.011	529.65	529.50	530.09
VNR06	5.6636E+02	3.4432E-01	7.4963E-01	2.2421E-01	-3.3094E+00	0.006	566.38	566.16	566.56
VNR07	6.7177E+02	-4.0534E-01	1.1152E+00	-1.8236E-01	4.7486E+00	0.018	671.93	671.73	672.55
VNR08	6.7198E+02	-5.0520E-01	6.5910E-01	2.4386E-01	5.1359E+00	0.017	672.10	671.91	672.67
VNR09	7.6357E+02	3.0504E-01	-2.5451E+00	-1.5900E+00	-4.8479E+00	0.007	763.28	762.68	763.58
VNR10	8.6725E+02	1.7793E+00	-1.3803E+01	-1.2226E+01	4.9354E+01	0.048	866.71	866.11	867.44
VNR11	8.6760E+02	2.0163E+00	-1.3424E+01	-1.4051E+01	4.8480E+01	0.034	867.08	866.46	867.90
VNP01	6.7191e+02	-3.3244e-01	1.2376e+01	1.2811e+00	-3.2838e+01	0.023	672.54	671.89	673.10
VNP02	8.6620e+02	-1.7438e+00	1.0498e+00	5.1759e+00	-5.6396e+00	0.007	866.22	865.85	866.63

Coefficients c0~c4, regression error, Average, Min and Max of center wavelengths of VNL (VNR-NP telescope -Left), VNN (VNR-NP telescope-Nadir), VNR (VNR-NP telescope-Right) and VNR-PL. The coefficients were calculated by EORC using original measurements by SGLI sensor team)

2.8 Mask/Flag

The first 0-1bits are common for the Level-2 products, input data lack and land/water flags. Others are defined as the right table.

Cloud masks are set by the target date, and the probably cloud is set by the multiple day tests. Bit-13 is set by additional cloud cover tests by polarization channels. Bit-14 (non-polarization) and 15 (polarization) are set when the grid is recovered by the pre-day's BRDF table.

The Level-3 statistics processing will use data with the QA_flag of bit-4, 7, 8, and 12=0 and the product value is within the valid range.

Table 5 Bit specification of QA_flag

bit	Description	Level-3 mask
0	no data (mask)	0
1	land (0: ocean, 1: land) (flag)	0
2	coast (flag)	0
3	sun-glint >0.005(flag)	0
4	sun-glint >0.12 (mask)	1
5	snow or ice (flag)	0
6	cloud (mask)	0
7	probably cloud (by multi-day) (flag)	1
8	high tau-a>0.8 (flag)	1
9	saturation recovery (flag)	0
10	BRF samples<=3(flag)	0
11	stray light (flag)	0
12	shadow (mask)	1
13	pol cloud or hi-tau (mask)	0
14	recovery by pre-days (flag)	0
15	recovery (pol) (flag)	0

3 Validation plan

3.1 Error budget estimation

3.1.1 TBD

3.2 Validation method after launch

3.2.1 Data release threshold accuracy：0.3 (≤443nm), 0.2 (>443nm) *

It is calculated as root mean square (RMS) difference (RMSD) between the instantaneous satellite estimates and in-situ measurements where AOT at 500nm less than 0.25

3.2.2 Standard accuracy：0.1 (≤443nm), 0.05 (>443nm) *

Same as the above

3.2.3 Target accuracy: 0.05 (≤443nm), 0.025 (>443nm) *

Same as the above

note: Defined with land reflectance~0.2, solar zenith<30deg, and flat surface

3.2.4 acquisition of validation data

In-situ data will be obtained mainly by the GCOM-C PIs at JAXA super site 500, JaLTER, JapanFlux, PEN sites and so on.

- Honda of Chiba Univ.（Spectral reflectance (incl. BRDF) data measured by FieldSpec, MS-720, Hyperspectral Camera from UAV, Spectral data measured from UAV. BiRS simulations will be used for uniform surfaces）、
- Nasahara of Tsukuba Univ.（PEN, Spectral data measured by MS-720 and MS-700 from Tower）

3.2.5 Comparison with MODIS BRDF product

Validation of special distribution and stability of the retrievals

4 Remaining issues

4.1 SGLI calibration sensitivities

- center-wavelength correction
- polarization sensitivity correction (applied after post-launch evaluation, especially for 380nm)

4.2 Validation of slope correction

Decision of application after evaluation of the improvement by the correction

4.3 Cloud detection evaluation and improvement

Validation and optimization of the cloud detection including cloud shadow

4.4 Use of LAI BRF model

It will be investigated after validation of the LAI model

4.5 Adjacent effect

The efficiency will be investigated after launch

They will be investigated with application researches in the future.

5 Additional output parameters

5.1 Photosynthetically active radiation (PAR)

PAR is included in the output file of the atmospheric correction, RSRF. The PAR algorithm is the same as the GLI PAR (Frouin 2004; Frouin and Murakami, 2007) and using the SGLI channels VN02, VN 03, VN 05, VN 08, and SW01.

5.2 Shortwave radiation (SWR)

SWR is included in the output file of the atmospheric correction, RSRF. The SWR algorithm is the same as the PAR, but the weighting coefficients of transmittance at the channels are optimized for SWR by using Pstar4 (Ota et al., 2010).

5.3 Polarization reflectance at PL01 and PL02

Surface Polarization reflectance, rp, at PL01 and PL02 are estimated by the observed polarization reflectance, rpo, Pstar4 atmospheric polarization, ra, and depolarization factor approximated by the square of the direct transmittance, trnb.

$rp=(rpo-ra)/(trnb^2)$

$rpo=sqrt(rq^2+ru^2)$; if(abs(ang).gt.pi/4) rpo=-rpo

ang=atan2(ru,rq)/2,

rq and ru are the Q and U component of the observed Stokes vector.

References

Ota, Y., A. Higurashi, T. Nakajima, and T. Yokota (2010), "Matrix formulations of radiative transfer including the polarization effect in a coupled atmosphere-ocean system," J. Quantitative Spectroscopy and Radiative Transfer, 111, 878-894.

Maignan, F., F.-M. Breon, R. Lacaze, Bidirectional reflectance of Earth targets: Evaluation of analytical models using a large set of spaceborne measurements with emphasis on the Hot Spot, Remote Sensing of Environment 90 (2004) 210–220.

Alexei I. Lyapustin, Yujie Wang, Istvan Laszlo, Thomas Hilker, Forrest G.Hall, Piers J. Sellers, Compton J. Tucker , Sergey V. Korkin: Multi-angle implementation of atmospheric correction for MODIS (MAIAC): 3. Atmospheric correction , Remote Sensing of Environment 127 (2012) 385–393.

Mahmoud El Hajj, Agnès Bégué, Bruno Lafrance, Olivier Hagolle, Gérard Dedieu and Matthieu Rumeau, Relative Radiometric Normalization and Atmospheric Correction of a SPOT 5 Time Series, Sensors 2008, 8, 2774-2791.

Olivier Hagolle, Gérard Dedieu, Bernard Mougenot, Vincent Debaecker, Benoit Duchemin, et al.. Correction of aerosol effects on multi-temporal images acquired with constant viewing angles: application to Formosat-2 images. Remote Sensing of Environment, Elsevier, 2008, 112(4), pp.1689-1701.

Frouin, R., Algorithm to estimate daily Photo-synthetically Available Radiation at the Ocean surface (OTSK14) , Nov.2004, https://suzaku.eorc.jaxa.jp/GLI/ocean/algorithm/ATBD_OTSK14_v210.pdf.

Frouin, R., and H. Murakami: Estimating photosynthetically available radiation at the ocean surface from ADEOS-II global imager data, J. Oceanography, 63,493-503, 2007.